

## Spin–Spin Coupling Tensors in Fluoromethanes

Perttu Lantto, Jaakko Kaski, Juha Vaara, and Jukka Jokisaari\*<sup>[a]</sup>

**Abstract:** All spin–spin coupling tensors  $\mathbf{J}$  of the fluoromethanes  $\text{CH}_3\text{F}$ ,  $\text{CH}_2\text{F}_2$ , and  $\text{CHF}_3$  are obtained theoretically by multiconfiguration self-consistent field linear response (MCSCF LR) ab initio calculations. Furthermore the principal values and the orientation of the principal axis systems of each theoretical  $\mathbf{J}$  tensor are specified. Experimental liquid crystal NMR (LC NMR) data on the tensorial properties of the CF spin–spin coupling in  $\text{CH}_3\text{F}$  and  $\text{CH}_2\text{F}_2$ , and the FF spin–spin coupling in  $\text{CHF}_3$  are also reported. In the analysis of the experiments, the contributions from molecular vibrations, as well as that of the correlation of vibrational and rotational motion to the experimental anisotropic couplings,  $D^{\text{exp}}$ , are taken into account. The information of the anisotropic indirect cou-

pling,  $\frac{1}{2}J^{\text{aniso}}$ , is detected as the difference between  $D^{\text{exp}}$  and the calculated dipolar coupling,  $D^{\text{calc}}$ . The extracted indirect contributions,  $\frac{1}{2}J^{\text{aniso}}$ , are in fair agreement with the ab initio results. All relative (experimental and theoretical) CF and FF indirect contributions,  $\frac{1}{2}J^{\text{aniso}}/D^{\text{exp}}$ , are negative and under 1.7% in magnitude, when the observed molecular orientations are used. Therefore, in the one bond CF couplings and in the two bond FF couplings, the indirect contribution can normally be ignored without introducing serious error to the determination of molecular orientation

and/or structure. However, a more accurate method is to partially correct for the indirect contribution by utilising the transferability of the spin–spin coupling tensors in related molecules. This is due to the fact that even small contributions may be significant, if the order parameter of the internuclear direction is negligibly small, leading to dominating indirect contributions. The very good agreement of the experimental values with the calculated coupling constants and the reasonable agreement in the anisotropic properties, which are experimentally much more difficult to define, indicates that the MCSCF LR method is capable of producing reliable  $\mathbf{J}$  tensors for these systems, contrary to the case of density-functional theory.

**Keywords:** ab initio calculations • fluoromethanes • liquid crystals • NMR spectroscopy • spin–spin couplings

### Introduction

In nuclear magnetic resonance (NMR) experiments performed in anisotropic liquid crystal (LC) phases or in the solid state, a contribution  $J_{ij}^{\text{aniso}}$  due to the anisotropic indirect nuclear spin–spin coupling tensor  $\mathbf{J}_{ij}$  appears combined with the direct dipolar coupling,  $D_{ij}$ , in the observable  $D_{ij}^{\text{exp}}$  coupling between the nuclei  $i$  and  $j$ .<sup>[1]</sup> As information on the molecular structure and orientation of the internuclear  $\mathbf{r}_{ij}$

vectors with respect to the magnetic field of the spectrometer is included in the  $D_{ij}$  couplings, the  $J_{ij}^{\text{aniso}}$  contribution should be small or known, when accurate structural or orientational data are wanted. For example, the recently introduced method of obtaining the direct  $^{13}\text{C}$ – $^{13}\text{C}$  couplings at natural abundance for LC molecules using two-dimensional double-quantum experiments relies on the smallness of the  $J_{ij}^{\text{aniso}}$  contribution.<sup>[2]</sup> For the carbon–carbon couplings,  $J_{\text{CC}}^{\text{aniso}}$  has been shown to be negligible regardless of the hybridisation of the carbon atoms.<sup>[3, 4]</sup> For the  $^1\text{H}$ – $^1\text{H}$  and  $^{13}\text{C}$ – $^1\text{H}$  couplings the same has been known to hold for already a long time.<sup>[1]</sup> Recent LC NMR experiments and ab initio calculations indicate non-negligible contributions to  $^5D_{\text{FF}}^{\text{exp}}$  and several types of  $D_{\text{CF}}^{\text{exp}}$  couplings in *para*-difluorobenzene.<sup>[5]</sup> An experimental study for the coupling anisotropy,  $\Delta J_{\text{CF}}$ , in  $\text{CH}_3\text{F}$  by applying solid-state NMR, gave only a coarse estimate for the quantity, because the information is masked by the broad lines of the spectrum.<sup>[6]</sup>

$^{19}\text{F}$  is an important spin- $\frac{1}{2}$  NMR nucleus due to its 100% natural abundance and high sensitivity, which make it easy to observe. Similarly to hydrogen, it is singly bonded in

[a] Prof. Dr. J. Jokisaari, P. Lantto, J. Kaski,<sup>[+]</sup> Dr. J. Vaara<sup>[++]</sup>  
Department of Physical Sciences, University of Oulu  
P. O. Box 3000, 90401 Oulu (Finland)  
Fax: (+358)8-553-1287  
E-mail: Jukka.Jokisaari@oulu.fi

[+] Present address:  
Raahe Institute of Computer Engineering  
Oulu Polytechnic  
P. O. Box 82, 90101 Oulu (Finland)

[++] Present address:  
Department of Chemistry  
University of Helsinki, P.O. Box 55  
00014 Helsinki (Finland)

molecules, which enables these two atoms to be exchanged. The  $^{13}\text{C}-^{19}\text{F}$  and  $^{19}\text{F}-^{19}\text{F}$  dipolar couplings are easily resolved by  $^1\text{H}$  irradiation. This is a frequently used method in case of large molecules, for which the  $^1\text{H}$  spectra are too complicated to be analyzed.<sup>[7, 8]</sup> However,  $J_{ij}^{\text{aniso}}$  is likely to be bigger in couplings involving fluorine than in the proton couplings, due to more complicated electronic structure of the former.<sup>[1]</sup> At the same time, electronic structure calculations are significantly more demanding for fluorine-containing molecules than for simple hydrocarbons.

$\text{CH}_3\text{F}$  is frequently investigated with the LC NMR method.<sup>[9–11]</sup> In the determination of dipolar couplings, the knowledge of the significance of using an accurate molecular geometry of the right type, appropriate liquid crystal solvents in the determination of dipolar couplings, vibrational corrections,<sup>[12, 13]</sup> and a model that takes into account the effects arising from orientation-dependent deformation<sup>[14]</sup> of the molecule, have made possible the accurate determination of  $\mathbf{J}$  tensors with LC NMR method.<sup>[15]</sup> In addition to this,  $\text{CH}_3\text{F}$  has been a subject for numerous theoretical investigations.<sup>[16–23]</sup> The coupling constants and especially the anisotropies of  $\mathbf{J}$  tensors are relatively far from the experimental

values in previous semi-empirical and coupled Hartree-Fock (CHF) level studies. Modern ab initio methods take into account all physical contributions to  $\mathbf{J}$  tensor and the triplet instability problem that occurs for some of the contributions, can be avoided using correlated wave functions. It is also possible to approach the basis set limit in these properties as proper basis sets are accessible with present computing facilities. These methodological developments allow one to revisit the classic problem using state-of-the-art experimental and theoretical methods. The trend in  $J_{ij}^{\text{aniso}}$  in fluorine couplings when the number of fluorine substituents increases is a subject of additional interest.

To establish the significance of the anisotropic fluorine spin–spin couplings in simple model systems, this paper reports multiconfiguration self-consistent field linear response (MCSCF LR) ab initio calculations<sup>[24]</sup> of the spin–spin coupling tensors in the  $\text{CH}_n\text{F}_{4-n}$  ( $n = 1, 2, 3$ ) series of molecules. We put special emphasis on obtaining reliable estimates for the  $\mathbf{J}_{\text{CF}}$ ,  $\mathbf{J}_{\text{HF}}$ , and  $\mathbf{J}_{\text{FF}}$  tensors, which, as fluorine has lone pairs, are known to be difficult for methods based on density-functional theory (DFT).<sup>[20, 21]</sup> Furthermore, LC NMR experiments were carried out by dissolving the molecules in selected nematic solvents in order to obtain the experimental information for comparison. In the latter process, the coupling corrections corresponding to the harmonic and anharmonic rovibrational motion as well as the deformational contributions arising from the correlation between vibrational and reorientational motions, were taken into account.

## Theory

The NMR spin Hamiltonian appropriate for spin- $1/2$  nuclei in molecules partially oriented in uniaxial LC solvents can be written in the high field approximation as

$$\hat{H} = -B_0/2\pi \sum_i \gamma_i (1 - \sigma_i) \hat{I}_{i,z} + \sum_{i < j} J_{ij} \hat{\mathbf{I}}_i \cdot \hat{\mathbf{I}}_j + \sum_{i < j} (D_{ij} + 1/2 J_{ij}^{\text{aniso}}) (3\hat{I}_{i,z} \hat{I}_{j,z} - \hat{\mathbf{I}}_i \cdot \hat{\mathbf{I}}_j) \quad (1)$$

where  $B_0$  is the magnetic field of the spectrometer (in the  $z$  direction of the laboratory-fixed frame),  $\gamma_i$ ,  $\hat{\mathbf{I}}_i$ , and  $\sigma_i$  are the gyromagnetic ratio, dimensionless spin operator, and nuclear shielding (sum of the isotropic and anisotropic contributions), of nucleus  $i$ , respectively. The dipolar coupling  $D_{ij}$  is defined as

$$D_{ij} = -P_2(\cos\theta) \frac{\mu_0 \hbar \gamma_i \gamma_j}{8\pi^2} \left\langle \frac{s_{ij}^{\text{D}}}{r_{ij}^3} \right\rangle \quad (2)$$

where  $\mu_0$  and  $\hbar$  have their usual meanings,  $r_{ij}$  is the length of the internuclear vector  $\mathbf{r}_{ij}$ , and  $s_{ij}^{\text{D}}$  is related to the order parameter (see below) of  $\mathbf{r}_{ij}$  with respect to LC director,  $\mathbf{n}$ .  $P_2$  is the second-order Legendre polynomial, and  $\theta$  the angle between  $\mathbf{B}_0$  and  $\mathbf{n}$ .

The experimentally observable anisotropic couplings can be partitioned as

$$D_{ij}^{\text{exp}} = D_{ij} + 1/2 J_{ij}^{\text{aniso}} = D_{ij}^{\text{eq}} + D_{ij}^{\text{h}} + D_{ij}^{\text{ah}} + D_{ij}^{\text{d}} + 1/2 J_{ij}^{\text{aniso}} \quad (3)$$

where  $D_{ij}^{\text{eq}}$  corresponds to the equilibrium geometry of the molecule, and  $D_{ij}^{\text{h}}$  and  $D_{ij}^{\text{ah}}$  are the contributions from the harmonic<sup>[12]</sup> and anharmonic<sup>[13]</sup> vibrations.  $D_{ij}^{\text{d}}$  is the defor-

**Abstract in Finnish:** Fluorimetäänien  $\text{CH}_3\text{F}$ ,  $\text{CH}_2\text{F}_2$  ja  $\text{CH}_3\text{F}$  spin–spin–kytkentätensorit  $\mathbf{J}$  on määritetty teoreettisesti käytäen multikonfiguraationaalisen aaltofunktion lineaarista vastetta (nk. MCSCF LR-menetelmä). Tensoreiden pääkomponentit ja pääakselisysteemit ilmoitetaan. Raportoimme myös nestekide-NMR-menetelmällä suoritettuja mittauksia C- ja F-ytimien välisen kytkennän tensoriominaisuuksille mono- ja difluorimetäänneissa, sekä F-ytimien välisen kytkennän vastaavia ominaisuuksia trifluorimetäänneissa. Koetulosten käsittelyssä on otettu huomioon molekyylin värähdysliikkeen sekä sen ja rotaatioliikkeen kytkentymisen vaikutus kokeellisiin anisotrooppisiin kytkentöihin  $D^{\text{exp}}$ . Epäsuoran anisotrooppisen kytkennän  $1/2 J^{\text{aniso}}$  vaikutus on määritetty kokeellisen ja lasketun dipolikytkennän erotuksesta  $D^{\text{exp}} - D^{\text{calc}}$ . Tuloksena saatavat epäsuorat kontribuutiot sopivat verrattain hyvin yhteen lasketujen ab initio -tulosten kanssa. Kokeellisesti ja teoreettisesti määritetyt CF- ja FF-kytkentöjen suhteelliset epäsuorat kontribuutiot  $1/2 J^{\text{aniso}}/D^{\text{exp}}$  ovat negatiivisia ja suuruudeltaan alle 1.7%, kun käytetään hyväksi mitattuja orientaatioparametreja. Siten yhden sidoksen CF- ja kahden sidoksen FF-kytkentöjen tapauksissa epäsuoran kontribuution huomiotta jättäminen on varsin pieni virhelähde molekyylin orientaation ja/tai rakenteen määrittämisessä. Tarkempi lähestymistapa on suorittaa osittainen korjaus käyttämällä hyväksi tietoa samankaltaisten molekyylien vastaavista spin–spin–kytkentätensoreista. Tämä johtuu siitä, että pienetkin epäsuorat kontribuutiot voivat dominoida tilanteessa, jossa ytimien välisen vektorin järjestysparametri lähestyy nollaa. Kokeellisten ja lasketujen kytkentävakioiden tapauksessa erinomainen ja—kokeellisesti huomattavasti vaikeampien—anisotrooppisten ominaisuuksien tapauksessa kohtuullisen hyvä yhteensopivuus osoittaa MCSCF LR-menetelmän käyttökelpoisuuden kytkentätensorien laskussa näille molekyylyleille, vastoin tiheysfunktioaaliteorian käytöstä saatuja kokemuksia.

mation contribution arising from the correlation between molecular vibration and rotation.<sup>[14]</sup> The experimental  $\frac{1}{2}J_{ij}^{\text{aniso}}$  is given by the difference between the experimental  $D_{ij}^{\text{exp}}$  and the calculated  $D_{ij} = D_{ij}^{\text{eq}} + D_{ij}^{\text{h}} + D_{ij}^{\text{ah}} + D_{ij}^{\text{d}}$  couplings. For the  $C_{2v}$  symmetry (e.g., difluoromethane) it can be decomposed as

$$J^{\text{aniso}} = \frac{2}{3}P_2(\cos\theta)[\Delta J S_{zz}^D + \frac{1}{2}(J_{xx} - J_{yy})(S_{xx}^D - S_{yy}^D)] \quad (4)$$

where  $z$  axis is parallel with the molecular symmetry axis. In the case of  $C_3$  or higher symmetry point group ( $\text{CH}_3\text{F}$  and  $\text{CHF}_3$ ) only the anisotropy,  $\Delta J = J_{zz} - \frac{1}{2}(J_{xx} + J_{yy})$ , contributes to Equation (4).

$$S_{\alpha\beta}^D = \langle s_{\alpha\beta}^D \rangle = \frac{1}{2}(3\cos\theta_{\alpha,\mathbf{n}}\cos\theta_{\beta,\mathbf{n}} - \delta_{\alpha\beta}) \quad (5)$$

In the Equation,  $S_{\alpha\beta}^D$  is the Saupe orientation tensor of the molecule. The angular brackets denote time averaging,  $\theta_{\alpha,\mathbf{n}}$  is the angle between the director  $\mathbf{n}$  of the LC phase and the  $\alpha$  axis of the molecule-fixed frame ( $x, y, z$ ).

If the  $D^{\text{exp}}$  couplings are determined in a narrow temperature range, they can be analyzed to a good accuracy based on the same average molecular geometry,  $r_a$ . However, when performing experiments within a wide temperature range the  $r_a$  geometry appears slightly temperature-dependent and, thus, the anharmonicity of the vibrational potential has to be considered in analyzing the NMR spectra. The information on the anisotropic properties of the  $\mathbf{J}$  tensors is combined with the molecular orientation tensor through Equation (4).  $J^{\text{aniso}}$  can be determined only if sufficient number of experimental couplings with known  $J^{\text{aniso}}$  is available to produce the necessary orientation information for the  $D^{\text{eq}}$ ,  $D^{\text{h}}$ ,  $D^{\text{ah}}$ , and  $D^{\text{d}}$  terms in Equation (3) of the interesting coupling. Each adjustable parameter of the equilibrium geometry requires at least one coupling. In addition, at least one coupling is needed in order to determine the anisotropy,  $\Delta A_{ij}$ , of the traceless interaction tensors,  $\mathbf{A}_{ij}$ , for each type of chemical bond of the molecule.<sup>[14]</sup> In the case of a strongly asymmetric  $\mathbf{A}_{ij}$ , another coupling is required for the asymmetry parameter of the tensor. In the present study we obtain information particularly on the  ${}^1\mathbf{J}_{\text{CF}}$  and  ${}^2\mathbf{J}_{\text{FF}}$  tensors, and similar features of these couplings in different molecules are discussed.

Using non-relativistic electronic structure theory, the spin–spin coupling tensor  $\mathbf{J}_{ij}$  is calculated as due to perturbations caused by nuclear magnetic moments (proportional to nuclear spins  $\mathbf{I}_i$ ). There are five different contributions arising from the terms of the perturbation Hamiltonian<sup>[25]</sup> that are linear both in  $\mathbf{I}_i$  and  $\mathbf{I}_j$ ,

$$\mathbf{J}_{ij} = \mathbf{J}_{ij}^{\text{PSO}} + \mathbf{J}_{ij}^{\text{FC}} + \mathbf{J}_{ij}^{\text{SD}} + \mathbf{J}_{ij}^{\text{FC}} + \mathbf{J}_{ij}^{\text{SD/FC}} \quad (6)$$

The diamagnetic spin-orbit tensor (DSO) is a reference state expectation value and thereby easy to calculate. The paramagnetic spin–orbit (PSO), spin–dipole (SD), Fermi contact (FC), and spin–dipole/Fermi contact cross term (SD/FC) tensors involve, in the Rayleigh–Schrödinger perturbation theory picture, sums over singlet (PSO) or triplet (SD, FC, SD/FC) excited states.<sup>[1]</sup> In terms of the response theory,<sup>[26]</sup> they can be expressed as linear response functions. Usually the main contribution to the anisotropic parts of the

$\mathbf{J}_{ij}$  tensor arises from the fully anisotropic SD/FC term, but the PSO and SD contributions cannot generally be neglected. The FC term is fully isotropic.

Besides that a reliable calculation of the SD, FC, and SD/FC tensors requires a reference state that is stable against triplet excitations, such as that provided by MCSCF or coupled cluster (CC) wave functions, the one-particle basis set has to be sufficiently flexible to enable good description of the atomic core region due to the  $r^{-3}$  or even  $\delta(r)$  (Dirac delta function) dependence of the relevant perturbation operators on the distance  $r$  between nucleus and electron. Systematic investigations of the rather stringent basis set requirements posed by the calculations of the spin–spin coupling were reported recently.<sup>[27, 28]</sup> Using the MCSCF method, the active space containing the correlated molecular orbitals (MOs) must be large enough so that dynamical correlation effects are sufficiently taken into account; a small active space typically leads to an overshoot of the correlation effects, similarly as observed in the second-order Møller–Plesset (MP2) perturbation theory calculations of nuclear shieldings.<sup>[29]</sup> In the realm of the MCSCF method, large restricted active space (RAS) wave functions are required for remedy.

## Calculations and Experiments

**ab initio Calculations:** MCSCF linear response calculations of the spin–spin coupling tensors, initially described by Vahtras et al.,<sup>[24]</sup> were performed applying the DALTON software.<sup>[30]</sup> We refer to the original paper and a recent review<sup>[29]</sup> for details.

In this work we have used basis sets originally due to Huzinaga<sup>[31]</sup> and further developed by Kutzelnigg and co-workers.<sup>[32]</sup> They are reasonably well-converged for spin–spin couplings, particularly when the size of the set is taken into account.<sup>[27]</sup> These so-called HII and HIII basis sets are shown in Table 1. Especially the HIII basis set is sufficient for good quality spin–spin couplings.

Table 1. Basis sets used in the MCSCF calculations.<sup>[a]</sup>

Basis	Element	Gaussian functions
HII	H	[5s1p/3s1p]
	C,F	[9s5p1d/5s4p1d]
HIII	H	[6s2p/4s2p]
	C,F	[11s7p2d/7s6p1d]

[a] Spherical Gaussians are used throughout. Only the innermost primitives of a given type are contracted.

We have used two balanced RAS type wave functions for each molecule, listed in Table 2. The active spaces were chosen by inspection of the MP2 natural orbital occupation numbers. The MP2 orbitals were used also as the starting point of the optimisation of the MCSCF wave function.<sup>[34]</sup> Since all the three molecules have only single bonds, no large static correlation effects are expected (at the equilibrium geometry) and therefore one anticipates little benefit from using multireference wave functions. Thus, we allowed only single and double excitations from all the occupied (in the SCF picture) valence molecular orbitals (MOs) to the virtual MOs.

We kept core MOs consisting of 1s atomic orbitals (AO) of carbon and fluorine inactive in the calculations. Therefore, there were two, three, and four inactive MOs in  $\text{CH}_3\text{F}$ ,  $\text{CH}_2\text{F}_2$ , and  $\text{CHF}_3$ , respectively. For  $\text{CH}_3\text{F}$ , 64.2% and 94.5% of all virtual MP2 particles were included in the MOs contained in the active space of RAS-I and RAS-II calculations, respectively. The RAS-I calculation was performed using both HII and HIII basis sets to monitor the basis set convergence. All (small) SD contributions, except for  ${}^1\mathbf{J}_{\text{CH}}$ , were carried over to the RAS-I/HIII

Table 2. MCSCF wave function used in the ab initio calculations.<sup>[a]</sup>

Molecule	Identifier	Wave function <sup>[b]</sup>	$n_{SD}$
CH <sub>3</sub> F	RAS-I	<sup>20</sup> RAS <sub>32</sub> <sup>32</sup>	1742
	RAS-II	<sup>20</sup> RAS <sub>16,9</sub> <sup>32</sup>	22042
CH <sub>2</sub> F <sub>2</sub>	RAS-I	<sup>2100</sup> RAS <sub>4321</sub> <sup>4321</sup>	3663
	RAS-II	<sup>2100</sup> RAS <sub>11,364</sub> <sup>4321</sup>	30755
CHF <sub>3</sub>	RAS-I	<sup>31</sup> RAS <sub>85</sub> <sup>85</sup>	23925
	RAS-II	<sup>31</sup> RAS <sub>16,12</sub> <sup>85</sup>	96193

[a] The identifier of the wave function and the number of the contained Slater determinants  $n_{SD}$  are shown. [b] The nomenclature inactiveRAS<sub>RAS3</sub><sup>RAS2</sup> is used.<sup>[33]</sup> CH<sub>3</sub>F and CHF<sub>3</sub> are calculated in the Abelian C<sub>s</sub> point group, and the two numbers in each category express the number of orbitals belonging to A' and A'' symmetry species. CH<sub>2</sub>F<sub>2</sub> is calculated in the C<sub>2v</sub> point group and the four numbers express orbitals belonging to A<sub>1</sub>, B<sub>2</sub>, B<sub>1</sub>, and A<sub>2</sub> symmetry species, respectively. For CH<sub>3</sub>F, the SCF wave function has seven and two orbitals occupied in the A' and A'' symmetries, respectively. The corresponding numbers for CHF<sub>3</sub> are 13 and 4. For CH<sub>2</sub>F<sub>2</sub>, the SCF wave function has six, four, two, and one orbitals in the A<sub>1</sub>, B<sub>2</sub>, A<sub>2</sub>, and B<sub>1</sub> symmetries.

calculation from the RAS-I/HII calculation; the SD contribution to <sup>1</sup>J<sub>CH</sub> was obtained from RAS-I/HIII calculation. The RAS-II calculation was performed with the HIII basis set to obtain reliable spin–spin coupling tensors.

The active spaces of the RAS-I and RAS-II calculations for CH<sub>2</sub>F<sub>2</sub> contain 68.0% and 94.5% of the virtual MP2 particles, respectively. The use of basis sets was similar to the case of CH<sub>3</sub>F. The SD contributions to all couplings were calculated in RAS-I level with the HII basis set.

Due to the number of the heavier atoms, the electronic structure of CHF<sub>3</sub> is complicated and the MP2 particles are distributed to several virtual orbitals, which made it more difficult than in the previous cases to find a large balanced active space. The RAS-I calculation employs an active space containing 69.7% of the virtual MP2 particles, while in RAS-II we utilise an active space that recovers 90.9% of the MP2 particles. Similar monitoring of the basis set convergence as in previous cases was not possible for CHF<sub>3</sub>, since the active space in RAS-II increased the computational effort considerably. This forced us to apply the HIII basis set only for the dominating contributions such as the FC and SD/FC terms. All contributions were calculated using both RAS-I and RAS-II active spaces for CHF<sub>3</sub>.

Finally, we list the equilibrium geometries of the molecules used in the calculations in Table 3. The geometry of difluoromethane (CH<sub>2</sub>F<sub>2</sub>) was theoretically optimised using the QCISD method<sup>[38]</sup> with the 6-311G(d,p) basis set in the Gaussian 94 program.<sup>[39]</sup>

**NMR experiments:** Gas-phase experiments were performed at the pressures of 0.8 atm, 5.0 atm, and 5.0 atm near room temperature for

Table 3. Molecular  $r_e$  geometries of CH<sub>3</sub>F, CH<sub>2</sub>F<sub>2</sub>, and CHF<sub>3</sub>.<sup>[a]</sup>

Molecule	Annotation <sup>[b]</sup>	$r_{CH}$	$r_{CF}$	$\angle HCH$	$\angle HCF$
CH <sub>3</sub> F	ZLI 1132	1.086 <sup>[d]</sup>	1.391	–	108.66
	Ref. [35] <sup>[c]</sup>	1.086	1.383	–	108.8
CH <sub>2</sub> F <sub>2</sub>	ZLI 1132	1.082	1.3508 <sup>[d]</sup>	112.78	109.15
	ZLI 1167	1.085	1.3508 <sup>[d]</sup>	112.60	109.21
	Phase V	1.066	1.3508 <sup>[d]</sup>	113.67	108.72
	Ref. [36]	1.084	1.3508	112.8	108.87
	Theor. <sup>[c,e]</sup>	1.092	1.354	112.9	108.8
CHF <sub>3</sub>	ZLI 1132	1.0958 <sup>[d]</sup>	1.3331 <sup>[d]</sup>	–	110.92
	ZLI 1167	1.0958 <sup>[d]</sup>	1.3331 <sup>[d]</sup>	–	110.66
	Ref. [37] <sup>[f]</sup>	1.0958	1.3331	–	110.32
	Ref. [37] <sup>[c]</sup>	1.0861	1.3309	–	110.28

[a] Bond lengths in Å and angles in degrees. [b] The LC solvent is given for the present experimental results, whereas a reference is given for geometries taken from the literature. [c] Used in the present ab initio calculations of **J** tensors. [d] Fixed. [e] Theoretical geometry from a QCISD/6–311G(d,p) calculation. [f] Experimental geometry tabulated in the reference.

<sup>13</sup>CH<sub>3</sub>F (99% <sup>13</sup>C-enrichment), CH<sub>2</sub>F<sub>2</sub>, and CHF<sub>3</sub>, respectively. In the LC NMR investigation, <sup>1</sup>H, <sup>13</sup>C, and <sup>19</sup>F-NMR spectra of di- and trifluoromethane, both at 8 atm, and monofluoromethane at 0.6 atm were measured. CHF<sub>3</sub> was dissolved in the thermotropic liquid crystals ZLI 1132 and ZLI 1167, CH<sub>2</sub>F<sub>2</sub> in ZLI 1132, ZLI 1167, and Phase V, and CH<sub>3</sub>F in ZLI 1132. The liquid crystals are products of Merck. The spectra were recorded on Bruker Avance DSX 300 and DRX 500 spectrometers and analysed with the PERCH software,<sup>[40]</sup> by using total line-shape analysis, which is assumed to be the most accurate method for simple spectra. The isotropic *J* coupling constants were determined at elevated temperatures where the LC solvents appear in the isotropic phase, and they were kept fixed in the analysis of the spectra taken from anisotropic phase at several temperatures.

In the least-squares fit of the molecular shape, **A**<sub>*ij*</sub> tensors, and the studied **J** tensor to the experimental data, the effects on dipolar couplings arising from the anharmonic and harmonic vibrations, and solvent-induced deformation were taken into account. This was performed by utilising the MASTER<sup>[41]</sup> and the AVIBR<sup>[13]</sup> programs. However, the former was used as a FMEX (Fortran–Matlab–Extension) subroutine in the Matlab program<sup>[42]</sup> and the latter was a version modified to include also the centrifugal distortion. For CH<sub>3</sub>F, the harmonic and anharmonic force fields were taken from references [43] and [44], respectively. For CH<sub>2</sub>F<sub>2</sub> and CHF<sub>3</sub>, we employed partial anharmonic force fields (containing the all-diagonal stretching force constants) estimated on the basis of harmonic force field with  $f_{rr} = -3af_{rr}$ , where  $a = 2 \text{ \AA}^{-1}$ .<sup>[45]</sup> The harmonic force fields for these molecules were adopted from reference [43].

## Results and Discussion

**ab initio Spin–spin coupling tensors:** The calculated spin–spin coupling constants and the anisotropies of the corresponding tensors for all the present molecules, along with the combination  $J_{xx} - J_{yy}$  for CH<sub>2</sub>F<sub>2</sub>, are given in Tables 4, 5, and 6.

**Monofluoromethane:** With the RAS-I calculation, the change in the spin–spin couplings and anisotropies when improving the basis set from HII to HIII is mostly within the range 0.4 to 8%, except 20% for  $\Delta^1 J_{CH}$ . Although this does not justify concluding that the basis set were converged, earlier application calculations and the recent systematic studies<sup>[27, 28]</sup> imply that the use of the HIII set gives reasonably good results. The deviation in the spin–spin coupling constants and anisotropies between RAS-I and RAS-II calculations is below 7% except 10% for <sup>1</sup>J<sub>CF</sub> and, for <sup>2</sup>J<sub>HH</sub>, even 23%. These changes are not surprising because the RAS3 orbital subspace is much larger in the RAS-II calculation than in the RAS-I calculation. The largest relative changes appear in the small couplings and anisotropies and so the absolute changes are reasonably small. With these observations and the earlier experience pointing out that the quite large RAS3 active space, such as the one in the RAS-II calculation, is sufficient for treating correlation for spin–spin coupling, we can say that the RAS-II approximation should be reliable. When improving the correlation treatment, the magnitude of the *J* couplings and anisotropies decreases in all cases except for <sup>1</sup>J<sub>CF</sub> and  $\Delta^1 J_{CH}$ .

Generally, FC is distinctly the most significant contribution in the coupling constants, whereas the SD/FC dominates the coupling anisotropies in monofluoromethane (Table 4). Cancellation of the DSO and PSO contributions occurs in all other parameters but <sup>2</sup>J<sub>HF</sub>, <sup>1</sup>J<sub>CF</sub>, and  $\Delta^1 J_{CF}$ , where the PSO gives a fairly large contribution. Also the DSO and SD

Table 4. Results of the MCSCF calculations for the spin–spin coupling tensors in CH<sub>3</sub>F.<sup>[a]</sup>

Method/Basis	Mechanism	$E+139$	$^1J_{CF}$	$\Delta^1J_{CF}$	$^1J_{CH}$	$\Delta^1J_{CH}$	$^2J_{HF}$	$\Delta^2J_{HF}$	$^2J_{HH}$	$\Delta^2J_{HH}$
RAS-II/HIII <sup>[b]</sup>	DSO		0.42	23.49	0.65	−7.64	−1.87	15.46	−3.02	−8.06
	PSO		35.20	−75.41	−0.15	7.70	11.79	−17.03	2.96	5.85
	SD		20.21	32.32	−0.24	0.16	−3.02	−3.09	0.38	−0.23
	FC		−212.39	−	141.22	−	41.88	−	−11.84	−
	SD/FC		−	227.44	−	5.89	−	−52.08	−	−8.09
RAS-I/HII	total	−0.271962	−154.01	220.56	148.84	7.16	51.08	−60.18	−15.99	−10.68
RAS-I/HIII <sup>[c]</sup>		−0.295151	−141.90	218.31	148.26	5.72	52.33	−59.06	−14.96	−11.01
RAS-II/HIII <sup>[b]</sup>		−0.443911	−156.56	207.84	141.49	6.10	48.78	−56.73	−11.52	−10.53
RAS-II/HIII <sup>[d]</sup>			−151.48	207.00	−	−	−	−	−	−
EOM-CCSD <sup>[e]</sup>			−174.48	−	138.38	−	46.48	−	−10.70	−
EOM-CCSD <sup>[f]</sup>			−169.56/−172.16	−	137.15/137.89	−	49.00/49.94	−	−9.82/−10.03	−
DFT			−258.50 <sup>[g]</sup> /−268.12 <sup>[h]</sup>	−	141.87 <sup>[g]</sup>	−	33.24 <sup>[g]</sup>	−	−2.76 <sup>[g]</sup>	−
CHF <sup>[i]</sup>			−97.5	263.6	172.8	4.7	66.6	−107.5	−30.0	−8.9
CNDO/2 <sup>[j]</sup>			−51.2	120.0	73.5	−10.8	8.9	−13.6	4.4	−
INDO <sup>[k]</sup>			−97	261	145	−19	−	−9	−	−
INDO <sup>[l]</sup>			−96.0	114.2	75.2	−11	7.3	−	−	−

[a] Calculations performed at the  $r_e$  geometry.<sup>[35]</sup> The anisotropy is defined as  $\Delta J = J_{zz} - \frac{1}{2}(J_{xx} + J_{yy})$  with the CF bond in the  $z$  direction. Results in Hz. The total energies of the calculations are also shown (in Ha). [b] The contributions of different physical mechanisms to the calculated tensors are indicated for the RAS-II/HIII calculation. The SD contribution to the  $^2J_{HH}$  tensor is taken from the RAS-I/HII calculation. [c] All SD contributions except for  $^1J_{CH}$  are from RAS-I/HIII calculation. [d] Estimate of vibrationally corrected values. [e] Ref. [23]. [f] Ref. [22]. [g] Ref. [21]. [h] Ref. [20]. [i] Ref. [19]. [j] Ref. [16]. [k] Ref. [17]. [l] Ref. [18].

Table 5. Results of the MCSCF calculations for the spin–spin coupling tensors in CH<sub>2</sub>F<sub>2</sub>.<sup>[a]</sup>

Property	DSO <sup>[b]</sup>	PSO <sup>[b]</sup>	SD <sup>[b]</sup>	FC <sup>[b]</sup>	SD/FC <sup>[b]</sup>	RAS-I/HII	RAS-I/HIII <sup>[c]</sup>	RAS-II/HIII <sup>[b,c]</sup>	DFT <sup>[d]</sup>	INDO <sup>[e]</sup>
$E+238$						−0.270338	−0.307872	−0.498176		
$^1J_{CF}$	0.76	−4.82	12.36	−229.01		−215.08	−202.00	−220.72	−343.11	−103.7
$\Delta^1J_{CF}$	0.54	46.46	−0.85		−35.76	9.50	10.94	10.39		6.9
$^1J_{CF,xx} - ^1J_{CF,yy}$	−16.06	−49.88	−10.02		−204.37	−280.47	−283.96	−280.33		
$^1J_{CH}$	1.13	−0.84	−0.17	175.56		183.43	183.30	175.67		
$\Delta^1J_{CH}$	−1.25	−0.45	0.33		−5.65	−6.65	−7.32	−7.02		
$^1J_{CH,xx} - ^1J_{CH,yy}$	14.68	−9.99	−0.59		−16.37	−15.33	−12.30	−12.26		
$^2J_{HF}$	−1.53	2.27	−3.51	54.65		54.03	55.57	51.88		
$\Delta^2J_{HF}$	7.49	4.25	2.22		−17.47	−4.55	−4.69	−3.51		
$^2J_{HF,xx} - ^2J_{HF,yy}$	−1.22	−6.27	−0.99		53.20	44.89	46.98	44.71		
$^2J_{HH}$	−2.61	2.57	0.50	−1.16		−4.32	−2.96	−0.69		
$\Delta^2J_{HH}$	−10.24	8.57	0.88		6.86	3.88	5.98	6.06		
$^2J_{HH,xx} - ^2J_{HH,yy}$	15.27	−11.01	0.71		11.67	16.98	16.94	16.65		
$^2J_{FF}$	−1.09	132.75	74.54	140.03		346.02	350.73	346.23		9.2
$\Delta^2J_{FF}$	−17.08	−267.66	−3.28		25.83	−251.56	−245.97	−262.19		−119.4
$^2J_{FF,xx} - ^2J_{FF,yy}$	−32.20	440.13	−113.45		−434.04	−196.31	−210.99	−139.55		

[a] All calculations performed at the  $r_e$  geometry. The anisotropy is defined as  $\Delta J = J_{zz} - \frac{1}{2}(J_{xx} + J_{yy})$  so that the  $z$  direction bisects the FCF angle with the fluorine atoms in the  $xz$  plane. Results in Hz. The total energies of the calculations are also shown (in Ha). [b] The contributions of different physical mechanisms to the calculated tensors are indicated for the RAS-II calculation. [c] The SD contributions from the RAS-I/HII calculation. [d] Ref. [20]. [e] Ref. [18].

Table 6. Results of the MCSCF calculations for the spin–spin coupling tensors in CHF<sub>3</sub>.<sup>[a]</sup>

Property	DSO <sup>[b]</sup>	PSO <sup>[b]</sup>	SD <sup>[b]</sup>	FC <sup>[b]</sup>	SD/FC <sup>[b]</sup>	RAS-I	RAS-II <sup>[b]</sup>	DFT <sup>[c]</sup>
$E+337$						−0.273433	−0.519782	
$^1J_{CF}$	1.19	−25.35	7.67	−225.58		−242.45	−242.07	−390.72
$\Delta^1J_{CF}$	−7.85	−35.01	−1.94		−128.54	−173.41	−173.34	
$^1J_{CH}$	1.72	−1.23	0.30	236.00		234.52	236.79	
$\Delta^1J_{CH}$	20.41	−9.75	−0.82		−41.03	−34.92	−31.19	
$^2J_{HF}$	−1.20	−0.09	−3.08	83.68		77.74	79.32	
$\Delta^2J_{HF}$	13.03	−8.23	−3.99		39.77	37.65	40.57	
$^2J_{FF}$	−0.80	−13.40	40.65	125.93		182.68	152.38	
$\Delta^2J_{FF}$	−16.78	−28.29	−24.27		−162.79	−235.47	−232.14	

[a] Calculations performed with the HII basis set at the  $r_e$  geometry.<sup>[37]</sup> The anisotropy is defined as  $\Delta J = J_{zz} - \frac{1}{2}(J_{xx} + J_{yy})$  with the CH bond in the  $z$  direction. Results in Hz. The total energies of the calculations are also shown (in Ha). [b] SD/FC and FC contributions calculated with the HIII basis set. The contributions of different physical mechanisms to the calculated tensors are indicated for the RAS-II calculation. [c] Ref. [20].

contributions are noteworthy in  ${}^1J_{CF}$  coupling. In  ${}^2J_{HH}$ , the cancellation of the nuclear spin-electron orbit mechanisms is not complete and the DSO gives a considerable contribution to  $\Delta^2J_{HH}$ .

The effect of vibrational motion on  ${}^1J_{CF}$  at 300 K was roughly estimated for  $CH_3F$ . A more complete method of treating the effects of the rovibrational motion on the isotropic and anisotropic properties was used in reference [46] in the case of the water molecule. The coupling and anisotropy of the  ${}^1J_{CF}$  tensor were approximated by the truncated Taylor series:

$$\langle P \rangle \approx P_e + \left( \frac{\partial P}{\partial r_{CF}} \right)_e (r_{CF} - r_{CF}^e)^{300K} + \frac{1}{2} \left( \frac{\partial^2 P}{\partial r_{CF}^2} \right)_e ((r_{CF} - r_{CF}^e)^2)^{300K} \quad (7)$$

of the desired property  $P$  in terms of the associated  $r_{CF}$  bond length only. The average linear and quadratic bond length extension at 300 K was obtained using the program AVIBR<sup>[13]</sup> with the same full cubic anharmonic force field as in reference [47]. This force field was also used in the analysis of the present experimental data. The vibrationally corrected values are listed in Table 4. Although the method is very approximate, it allows assessing the need of performing rovibrational corrections to achieve sufficient accuracy. The corresponding changes from equilibrium values in  ${}^1J_{CF}$  and  $\Delta^1J_{CF}$  are  $-3.2\%$  and  $-0.4\%$ , respectively. These changes are of the same order of magnitude as the difference due to using different basis set and correlation treatment. As a conclusion, the vibrational motion does not seem to have any dramatic effect on the comparison of the theoretical and experimental values in the case of  ${}^1J_{CF}$  tensor.

Table 7 compares our best calculations of the coupling constants with the experiment. It can be seen that the RAS-II/HIII calculation underestimates both the CF and CH couplings over one bond by about 4% and the HF coupling over two bonds by 5%, when comparing with the experimental gas phase spin-spin coupling constants. It is justified to claim the

Table 7. Theoretical and experimental spin-spin coupling constants for  $CH_3F$ ,  $CH_2F_2$ , and  $CHF_3$ .

Molecule	Method	${}^1J_{CF}$	${}^1J_{CH}$	${}^2J_{HF}$	${}^2J_{FF}$	${}^2J_{HH}$
$CH_3F$	RAS-II/HIII	-156.6	141.5	48.8	-	-11.5
	RAS-II/HIII <sup>[a]</sup>	-151.48				
	LC/ZLI 1132 <sup>[b]</sup>	-161.30(4)	149.19(3)	46.34(3)		
	GAS <sup>[c]</sup>	-163.00(2)	147.25(2)	46.47(2)		
	GAS	-160.2 <sup>[d]</sup>		46.6 <sup>[e]</sup>		
	PURE LIQ. <sup>[f]</sup>	-160.8	149.15	46.3		
$CH_2F_2$	SOLID <sup>[g]</sup>	-158				
	RAS-II/HIII	-220.7	175.7	51.9	346.2	-0.7
	LC/ZLI 1167 <sup>[h]</sup>	-236.01(5)	183.95(5)	50.26(4)		
	LC/ZLI 1132 <sup>[i]</sup>	-236.065(2)	184.049(2)	50.3013(12)		
	LC/Phase V <sup>[j]</sup>	-236.186(6)	184.024(7)	50.253(5)		
	GAS/5 atm <sup>[k]</sup>	-233.91(11)	180.38(4)	49.06(13)		
$CHF_3$	GAS	-232.7 <sup>[d]</sup>		50.09 <sup>[e]</sup>		
	RAS-II/HIII	-242.1	236.8	79.3	152.4	-
	LC/ZLI 1167 <sup>[k]</sup>	-276.801(9)	242.65(2)	79.300(7)		
	LC/ZLI 1132 <sup>[l]</sup>	-277.03(2)	242.13(9)	79.292(9)		
	GAS <sup>[c]</sup>	-272.18(7)	235.26(9)	79.56(2)		
	GAS	-272.4 <sup>[d]</sup>		79.75 <sup>[e]</sup>		

[a] Vibrationally corrected value. [b] Present experiments at 350 K. [c] Present experiments. [d] Ref. [48]. [e] Ref. [49]. [f] Ref. [10]. [g] Ref. [6]. [h] Present experiments at 345 K. [i] Present experiments at 330 K. [j] Present experiments at 340 K. [k] Present experiments at 349 K. [l] Present experiments at 345 K.

agreement to be excellent, although we note that the ab initio calculations should be performed at the  $r_\alpha$  geometry instead of  $r_e$  geometry (as done presently) to be fully comparable with the experiments. As a conclusion, the high accuracy of the coupling constants allows also the anisotropies to be considered reliable.

There are many theoretical calculations of  $\mathbf{J}$  tensors for fluoromethanes, especially for  $CH_3F$ , but our values of the anisotropic parts are unique among the modern work. For monofluoromethane the spin-spin couplings constants have been calculated at the first principles level by CHF,<sup>[19]</sup> DFT,<sup>[20, 21]</sup> and equation-of-motion coupled cluster singles and doubles (EOM-CCSD)<sup>[22, 23]</sup> methods. Both these and the semi-empirical results are collected to Table 4. One should notice that DFT has problems in describing other than the CH coupling (141.87 Hz).<sup>[21]</sup> It clearly overestimates the magnitude of the CF coupling ( $-258.50$  Hz) and underestimates the HF (33.24 Hz) and HH ( $-2.76$  Hz) couplings. This is very different from the case of hydrocarbons where the DFT method has been shown to be very successful.<sup>[50]</sup> This controversial behavior has already been discussed by Malkina et al.,<sup>[20]</sup> it appears that the deficiencies of the exchange-correlation functionals deteriorate the performance of the DFT in couplings involving atoms with lone pairs such as fluorine. The EOM-CCSD method, on the other hand, works very well and the values are close to experimental ones, although the present values are slightly closer for the CF and CH couplings. The literature reports one CHF level<sup>[19]</sup> and a few semi-empirical<sup>[16-18]</sup> calculations concerning the anisotropic properties of the  $\mathbf{J}$  tensors of monofluoromethane. As the CHF calculations give coupling constants that are far away from the experimental couplings, the good agreement of the anisotropies with the present results is likely to be coincidental, especially as the CHF method does not take the electron correlation into account and the modest basis set used can not describe the core region correctly. The semi-empirical coupling constants are far from the experimental values and it is not surprising that the anisotropic properties are even more incorrect; they give wrong sign for  $\Delta^1J_{CH}$ , and  $\Delta^1J_{CF}$  seems to be even more sensitive to the choice of the parameters. Also  $\Delta^2J_{HF}$  changes from the semi-empirical value of  $-9$  Hz<sup>[18]</sup> to the CHF value of  $-107.5$  Hz.<sup>[19]</sup> Our present results for all couplings seem to be the best available self-supporting data.

**Difluoromethane:** The basis set convergence was examined at the RAS-I wave function level. The absolute changes from HII to HIII are fairly small, which implies that the basis set convergence is satisfactory. The differences in  $\mathbf{J}$  tensors between RAS-I and RAS-II calculations are very similar to monofluoromethane. In the case of  $CH_2F_2$ , the biggest changes are 77% for the generally difficult  ${}^2J_{HH}$ , 25% for  $\Delta^2J_{HF}$ , and 34% for  ${}^2J_{FF,xx} - {}^2J_{FF,yy}$ . In the first two couplings the absolute change in Hz is small but in the last one the change is considerable, that is 71.44 Hz, and the coupling is not necessarily fully converged. Nevertheless, the overall results can be considered quite reliable. The magnitude of most of the isotropic and anisotropic properties of the  $\mathbf{J}$  tensors (with the exceptions  ${}^1J_{CF}$ ,  $\Delta^2J_{HH}$ , and  $\Delta^2J_{FF}$ ) decreases as the wave function is improved.

Also in the case of difluoromethane, the FC and SD/FC contributions are the dominant ones for  $J$  coupling constants and anisotropies, respectively. However, for anisotropic properties of  ${}^2\mathbf{J}_{\text{FF}}$ , PSO is the main contribution and  ${}^2J_{\text{FF}}$  obtains almost equal contributions from the PSO, SD, and FC terms. PSO is a significant contribution to anisotropic properties of  ${}^1\mathbf{J}_{\text{CF}}$ , too.

The best calculation, RAS-II/HIII, underestimates the magnitude of the  ${}^1J_{\text{CF}}$  and  ${}^1J_{\text{CH}}$  about 6% and 3%, respectively. As also the theoretical  ${}^1J_{\text{HF}}$  is only about 6% bigger than the experimental result, and the two-bond couplings are known to be difficult to calculate reliably,<sup>[27, 28]</sup> the calculated tensors for all couplings can be considered to be very satisfactory.

The only first principles calculation of spin–spin couplings for difluoromethane is the DFT work by Malkina et al.<sup>[20]</sup> The only reported value,  ${}^1J_{\text{CF}} = -343.11$  Hz, differs by over 100 Hz from the experimental value. This overestimation, although it is a rather systematic one, is harmful for detailed molecular structure determination as it implies also a large error in the anisotropy of  $\mathbf{J}$  tensor. In earlier semi-empirical work, Nakatsuji et al.<sup>[18]</sup> estimated the anisotropies  $\Delta^1J_{\text{CF}} = 6.9$  Hz and  $\Delta^1J_{\text{FF}} = -119.4$  Hz that, despite the correct signs, are clearly underestimations of the magnitude.

**Trifluoromethane:** The calculations of trifluoromethane were very time-consuming. We assume that the basis set convergence is similar to that in  $\text{CH}_3\text{F}$  and  $\text{CH}_2\text{F}_2$ . This means that the use of the HII set for  $\text{CHF}_3$  is a slight compromise, although the dominant and most basis set sensitive contributions, FC and SD/FC, were calculated using the HIII set. Upon this partial upgrade of the basis, the  ${}^1J_{\text{CF}}$ ,  $\Delta^1J_{\text{CH}}$ , and  $\Delta^2J_{\text{FH}}$  seem to be the most sensitive quantities: the changes are 6%, 11%, and 8%, respectively. Other quantities differ less than 2%. The same arguments as before are valid also in this case and the best calculation is therefore fairly well converged for the basis set part.

The changes from the RAS-I active space to RAS-II are generally below 3% in  $J$  couplings and anisotropies, but for the CF coupling the difference is 6% and, for FF, 18%. This indicates that the couplings between the heavier atoms such as C and F necessitate a particularly good correlation treatment, whereas all the molecules in this study imply that couplings to H are most sensitive to the inadequacies in the basis set. The anisotropic properties of the  $\mathbf{J}$  tensors are well-converged and as the active space is also in this case quite large, it is justified to claim that the RAS-II correlation treatment for trifluoromethane is a good one. The magnitudes of the  ${}^1J_{\text{CH}}$ ,  ${}^2J_{\text{HF}}$ , and  $\Delta^2J_{\text{HF}}$  increase, while the other  $\mathbf{J}$  tensor properties decrease as the wave function is improved.

SD gives a reasonably large contribution to  ${}^2J_{\text{FF}}$ , while  $\Delta^1J_{\text{CH}}$ , and  $\Delta^1J_{\text{CF}}$  are very dependent on the DSO and PSO contributions, respectively. The main contributions are still the FC and SD/FC in all couplings. Trifluoromethane is a good example of the fact that all contributions have to be taken into account in the calculations of the spin–spin coupling tensors.

Comparison of the best theoretical calculation, RAS-II/HIII, with the experimental spin–spin coupling constants reveals excellent agreement for  ${}^1J_{\text{CH}}$  and  ${}^2J_{\text{HF}}$ . The calculation

underestimates the magnitude of the  ${}^1J_{\text{CF}}$  by about 11% but even that accuracy implies that also the theoretical anisotropies are near the true ones. Previous theoretical calculations of the  $\mathbf{J}$  tensors in trifluoromethane are rare. The only available value,  ${}^1J_{\text{CF}} = -390.72$  Hz, was obtained with the DFT method.<sup>[20]</sup>

Tables 8, 9, and 10 list the theoretical principal values and orientation of the principal axis systems (PAS) of the  $\mathbf{J}$  tensors for  $\text{CH}_3\text{F}$ ,  $\text{CH}_2\text{F}_2$ , and  $\text{CHF}_3$ , respectively. The molecule-fixed coordinate frames and the principal axes of the  $\mathbf{J}$  tensors for  $\text{CH}_3\text{F}$ ,  $\text{CH}_2\text{F}_2$ , and  $\text{CHF}_3$  are presented in Figures 1, 2, and 3, respectively.

Table 8. Theoretical principal values and the orientation of the principal axis system of the spin–spin coupling tensors in  $\text{CH}_3\text{F}$ .<sup>[a]</sup>

	$J_{33}$	$J_{22}$	$J_{11}$
${}^1\mathbf{J}_{\text{CF}}$ <sup>[b]</sup>	–225.84	–225.84	–18.00
${}^1\mathbf{J}_{\text{CH}}$ <sup>[c]</sup>	152.62	149.84	122.00
${}^2\mathbf{J}_{\text{HF}}$ <sup>[d]</sup>	100.76	37.00	8.59
${}^2\mathbf{J}_{\text{HH}}$ <sup>[e]</sup>	–20.41	–7.78	–6.36

[a] Principal values in Hz. Values have been ordered as  $|J_{33}| \geq |J_{22}| \geq |J_{11}|$ . [b]  $J_{11}$  is directed along the CF bond direction and  $J_{33}$  is in the FCH plane. [c] Both  $J_{33}$  and  $J_{11}$  are in the HCF plane. The direction of  $J_{11}$  makes an angle of  $9.9^\circ$  with the CH bond direction. [d] Both  $J_{33}$  and  $J_{11}$  are in the HCF plane. The direction of  $J_{11}$  makes an angle of  $9.2^\circ$  with the CF bond direction. [e]  $J_{11}$  makes an angle of  $7.8^\circ$  with the HH direction and is practically in the HCH plane.  $J_{33}$  makes an angle of  $33.9^\circ$  with the HCH plane and the angle with the HH direction is  $96.8^\circ$ .

Table 9. Theoretical principal values and the orientation of the principal axis system of the spin–spin coupling tensors in  $\text{CH}_2\text{F}_2$ .<sup>[a]</sup>

	$J_{33}$	$J_{22}$	$J_{11}$
${}^1\mathbf{J}_{\text{CF}}$ <sup>[b]</sup>	–364.34	–261.19	–36.62
${}^1\mathbf{J}_{\text{CH}}$ <sup>[c]</sup>	186.00	184.15	156.88
${}^2\mathbf{J}_{\text{HF}}$ <sup>[d]</sup>	87.38	45.38	22.87
${}^2\mathbf{J}_{\text{HH}}$ <sup>[e]</sup>	–11.04	5.61	3.35
${}^2\mathbf{J}_{\text{FF}}$ <sup>[f]</sup>	503.40	363.84	171.43

[a] Principal values in Hz. Values have been ordered as  $|J_{33}| \geq |J_{22}| \geq |J_{11}|$ . [b]  $J_{11}$  makes an angle of  $8.3^\circ$  with the CF bond direction.  $J_{33}$  is directed perpendicular to the FCF plane. [c] Both  $J_{33}$  and  $J_{11}$  are in the HCH plane.  $J_{11}$  makes an angle of  $12.3^\circ$  with the CH bond. [d]  $J_{33}$  makes an angle of  $1.8^\circ$  with the HCF plane towards the other F atom and  $44.2^\circ$  with the HF direction.  $J_{11}$  makes an angle of  $45.9^\circ$  with the HF direction and  $4.8^\circ$  with the HCF plane towards the other H. [e]  $J_{22}$  is directed along the HH direction.  $J_{33}$  is directed perpendicularly to the HCH plane. [f]  $J_{33}$  is directed along the FF direction.  $J_{22}$  is directed perpendicularly to the FCF plane.

Table 10. Theoretical principal values and the orientation of the principal axis system of the spin–spin coupling tensors in  $\text{CHF}_3$ .<sup>[a]</sup>

	$J_{33}$	$J_{22}$	$J_{11}$
${}^1\mathbf{J}_{\text{CF}}$ <sup>[b]</sup>	–387.25	–333.49	–5.47
${}^1\mathbf{J}_{\text{CH}}$ <sup>[c]</sup>	247.18	247.18	216.00
${}^2\mathbf{J}_{\text{HF}}$ <sup>[d]</sup>	107.11	70.67	60.17
${}^2\mathbf{J}_{\text{FF}}$ <sup>[e]</sup>	417.26	189.61	–149.72

[a] Principal values in Hz. Values have been ordered as  $|J_{33}| \geq |J_{22}| \geq |J_{11}|$ . [b] Both  $J_{33}$  and  $J_{11}$  are in the HCF plane.  $J_{11}$  makes an angle of  $4.1^\circ$  with the CF bond direction. [c]  $J_{11}$  is directed along the CH bond direction and  $J_{33}$  is in the HCF plane. [d] Both  $J_{33}$  and  $J_{11}$  are in the HCF plane.  $J_{33}$  makes an angle of  $7.2^\circ$  with the CH bond direction. [e]  $J_{33}$  is directed along the FF direction.  $J_{11}$  makes an angle of  $12.3^\circ$  with the FCF plane in question.

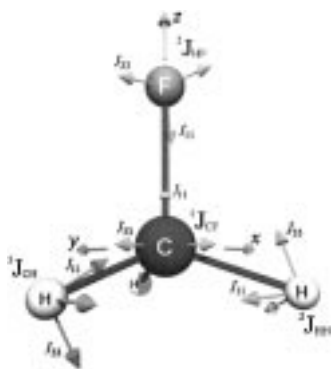


Figure 1. Principal axis systems of the spin–spin coupling tensors in  $\text{CH}_3\text{F}$ . The  ${}^2J_{\text{HF}}$  and  ${}^2J_{\text{HH}}$  couplings are to the proton in the  $xz$  plane (in the foreground).

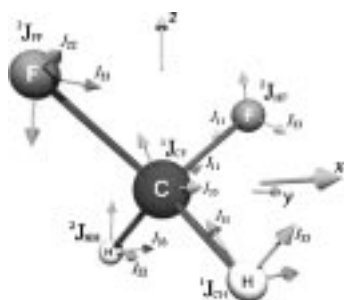


Figure 2. Principal axis systems of the spin–spin coupling tensors in  $\text{CH}_2\text{F}_2$ . The  ${}^2J_{\text{HF}}$  coupling is to the proton with the positive  $x$ -coordinate value (in the foreground).

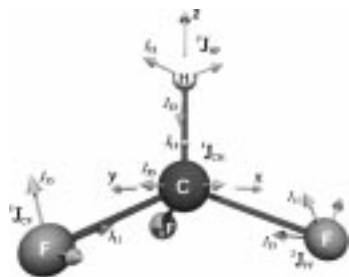


Figure 3. Principal axis systems of the spin–spin coupling tensors in  $\text{CHF}_3$ . The  ${}^2J_{\text{HF}}$  coupling is to the fluorine in the  $xz$  plane (in the foreground) while the  ${}^2J_{\text{FF}}$  coupling is to the fluorine with the positive  $y$ -coordinate value (in the background).

**NMR results:** Disregarding the possible medium effects, the experimental  $J$  couplings form a good test of the ab initio calculations, as they can be determined very accurately in experiments. However, the gas-to-isotropic solution change is clear in  ${}^1J_{\text{CH}}$  and  ${}^1J_{\text{CF}}$  (see Table 7).  ${}^1J_{\text{CH}}$  increases 1.3% in  $\text{CH}_3\text{F}$ , 2.0% in  $\text{CH}_2\text{F}_2$ , and 3.2% in  $\text{CHF}_3$ , whereas  ${}^1J_{\text{CF}}$  changes by about  $-1.3$ ,  $0.9$ , and  $1.8\%$ , respectively, indicating slight changes in molecular geometry and/or electronic structure. For this reason, we used several measurement temperatures for each sample instead of measuring several samples at one temperature. The solvent effects are assumed to be similar in one solvent. Thus the molecular equilibrium ( $r_e$ ) geometry was constrained to be the same in analysing the full data set obtained from one sample. The  $D^{\text{exp}}$  couplings of the different samples were independently accounted for, but the  $\Delta J$  values for a molecule in different surroundings were

assumed to be the same. This is quite a safe approximation according to ab initio results ( $\Delta{}^1J_{\text{CF}}$  changes only by a few Hz with an acceptable change in the  $r_{\text{CF}}$  bond length of  $\text{CH}_3\text{F}$ ). The experimental dipolar couplings are given in Table 11.

The  $\mathbf{A}_{ij}$  tensors, fitted to the  $D^{\text{exp}}$  couplings, define the torques acting on the  $ij$  bonds of the molecule. The sum of the  $\mathbf{A}_{ij}$ 's in the molecule-fixed frame determines the solvent-induced interaction tensor,  $A_{\alpha\beta}$ ,<sup>[14]</sup> that is a function of the orientation of the solute molecule with respect to the LC director.  $A_{\alpha\beta}$  represents the molecular interaction potential that couples with the molecular vibrational potential; as a result, the molecular rotation and vibration are correlated leading to deformational contributions to  $D^{\text{exp}}$  couplings. Simultaneously, the interaction potential leads to non-zero molecular average orientation and, usually, to the dominant contribution ( $D^{\text{eq}}$ ) to  $D^{\text{exp}}$ .

In the bond-additivity model used,<sup>[14]</sup> one principal component,  $A_{ij,L}$ , is assumed to be in the  $\mathbf{r}_{ij}$  direction. In this bond-fixed basis, the transverse and vertical components,  $A_{ij,T}$  and  $A_{ij,V}$ , respectively, are equal for  $\mathbf{A}_{\text{CF}}$  in  $\text{CH}_3\text{F}$  and for  $\mathbf{A}_{\text{CH}}$  in  $\text{CHF}_3$  due to the local symmetry of the bond. On the contrary, the asymmetry parameter,  $\eta_{ij} = (A_{ij,T} - A_{ij,V})/A_{ij,L}$ , is found to be non-negligible for  $\mathbf{A}_{\text{CH}}$  in  $\text{CH}_3\text{F}$ , for  $\mathbf{A}_{\text{CH}}$  and  $\mathbf{A}_{\text{CF}}$  in  $\text{CH}_2\text{F}_2$ , and for  $\mathbf{A}_{\text{CF}}$  in  $\text{CHF}_3$ .  $\text{CHF}_3$  possesses a particularly large  $\eta_{\text{CF}}$  in the LC solvents used, being due to the small  $A_{ij,L}$ . The  $\eta$  values are much smaller in  $\text{CH}_2\text{F}_2$  and  $\text{CH}_3\text{F}$ , that is between  $-1.7$  and  $0.2$  in the different solvents. The  $\Delta A_{\text{CH}}$  and  $\Delta A_{\text{CF}}$  values range typically from  $-1$  to  $1$  (in units of  $10^{-21}$  J) and from  $1$  to  $2$ , respectively. As an example, the principal components of the  $\mathbf{A}_{\text{CF}}$  tensors of the molecules in the ZLI 1132 solvent at 300 K (except for  $\text{CHF}_3$  at 305 K) are shown in Figure 4, where the transverse components are in the HCF symmetry plane for  $\text{CH}_3\text{F}$  and  $\text{CHF}_3$ , and in the FCF plane for  $\text{CH}_2\text{F}_2$ .

The correlation between rotational and vibrational motions—manifested by deformation contributions to direct couplings—is surprisingly important in the case of  $\text{CHF}_3$  dissolved in the ZLI 1132 liquid crystal. The experimental dipolar couplings change sign at about 321 K, except for  ${}^1D_{\text{CH}}$  that vanishes near 325 K. In Equation (3), the  $D^{\text{eq}}$ ,  $D^{\text{h}}$ ,  $D^{\text{ah}}$ , and  $1/2 J^{\text{aniso}}$  terms are directly proportional to the orientational order parameter,  $S_{zz} = S_{\text{CH}}$ , of the molecule. Only the  $D^{\text{d}}$  term can be non-zero with the average orientation  $S_{zz} = 0$  in uniaxial anisotropic surroundings. At 321 K, the interpolated  ${}^2D_{\text{HF}}$ ,  ${}^2D_{\text{FF}}$  and  ${}^1D_{\text{CF}}$  values are very close to zero, whereas  ${}^1D_{\text{CH}}$  is between  $-25$  and  $-30$  Hz. This non-zero coupling is due to rovibrational effects that are, for example, also responsible for the dipolar couplings of methane, for which the other terms but  $D_{ij}^{\text{d}}$  in Equation (3) are zero due to the molecular symmetry.<sup>[14]</sup> The contribution is remarkable also at other temperatures, as seen in Table 12, where the dipolar couplings together with their contributions for each molecule dissolved into the liquid crystal ZLI 1132 are shown as an example.

The resolved molecular  $r_e$  geometries, given in Table 3, appear slightly solvent-dependent. Probably the “best  $r_e$  geometry”, given by the LC NMR method, is obtained by using the LC solvent mixtures where the  ${}^1D_{\text{CH}}$  coupling of methane vanishes.<sup>[51]</sup> Presently, however, the non-disturbed



Table 11. Experimental dipolar couplings at different temperatures.<sup>[a]</sup>

Molecule	<i>T</i> /K	<sup>1</sup> <i>D</i> <sub>CF</sub>	<sup>1</sup> <i>D</i> <sub>CH</sub>	<sup>2</sup> <i>D</i> <sub>HF</sub>	<sup>2</sup> <i>D</i> <sub>FF</sub>	<sup>2</sup> <i>D</i> <sub>HH</sub>	
<b>CH<sub>3</sub>F</b>	<b>ZLI 1132</b>						
	240	–1119.660(15)	817.47(4)	–880.62(4)		1097.40(2)	
	260	–1029.369(5)	751.713(5)	–809.304(5)		1008.496(3)	
	275	–934.653(4)	682.689(2)	–734.523(2)		915.2602(13)	
	290	–836.420(4)	611.237(3)	–657.163(3)		818.8159(14)	
	300	–767.915(6)	561.254(3)	–603.123(3)		751.441(2)	
	310	–694.083(13)	507.50(2)	–545.02(2)		678.993(12)	
	320	–612.982(10)	448.348(7)	–481.185(7)		599.470(4)	
	330	–513.42(2)	375.795(5)	–403.024(5)		502.028(3)	
<b>CH<sub>2</sub>F<sub>2</sub></b>	<b>ZLI 1132</b>						
	260	–449.981(6)	968.277(9)	–180.416(7)	–457.740(4)	1478.271(6)	
	270	–439.134(3)	944.378(4)	–164.453(6)	–465.515(2)	1411.835(3)	
	280	–423.765(3)	910.403(4)	–148.847(4)	–464.963(2)	1334.988(3)	
	290	–403.906(5)	867.060(6)	–133.947(4)	–455.839(3)	1250.433(4)	
	300	–377.441(3)	809.698(4)	–118.589(4)	–436.457(2)	1150.087(3)	
	310	–342.815(3)	735.104(5)	–102.574(2)	–404.543(2)	1030.345(3)	
	320	–291.607(4)	625.12(2)	–83.408(3)	–350.157(2)	866.009(11)	
	<b>CH<sub>2</sub>F<sub>2</sub></b>	<b>ZLI 1167<sup>[b]</sup></b>					
295		–450.561(10)	972.41(2)	–148.58(2)	–509.783(7)	1393.291(10)	
300		–432.815(11)	932.68(2)	–139.84(2)	–494.162(7)	1330.026(10)	
305		–416.946(8)	897.70(2)	–131.94(2)	–480.546(6)	1273.574(10)	
310		–401.113(8)	863.21(2)	–124.36(2)	–466.480(6)	1218.174(9)	
315		–384.250(6)	826.47(2)	–116.78(2)	–450.569(4)	1160.451(10)	
320		–365.941(8)	786.53(2)	–109.19(2)	–432.301(5)	1099.225(9)	
325		–344.84(3)	741.18(2)	–101.27(2)	–410.120(6)	1031.395(13)	
330		–319.57(3)	686.22(3)	–92.38(3)	–381.78(2)	951.46(2)	
335		–287.31(4)	616.34(5)	–81.99(4)	–344.66(4)	851.88(3)	
338		–260.19(4)	559.40(5)	–74.03(5)	–313.27(2)	771.82(4)	
<b>CH<sub>2</sub>F<sub>2</sub></b>		<b>Phase V</b>					
		255	–476.041(4)	1031.620(5)	–9.262(4)	–775.751(3)	1060.425(4)
	265	–450.446(3)	975.330(3)	–8.576(2)	–733.875(2)	1002.012(2)	
	275	–423.996(2)	917.346(3)	–8.138(2)	–690.2379(11)	942.565(2)	
	285	–395.272(2)	854.574(3)	–7.879(2)	–642.6221(13)	878.729(2)	
	290	–379.142(2)	819.714(3)	–7.788(2)	–615.8315(15)	843.418(2)	
	295	–362.259(2)	782.708(2)	–7.712(2)	–587.7905(15)	806.0056(12)	
	300	–343.705(5)	742.685(5)	–7.637(4)	–557.018(3)	765.560(3)	
<b>CHF<sub>3</sub></b>	<b>ZLI 1132</b>						
	287.5	99.163(2)	–464.77(2)	68.55(2)	–112.56(2)		
	305	38.259(2)	–196.91(2)	26.47(2)	–43.58(2)		
	315	12.865(2)	–83.67(2)	8.81(2)	–14.80(2)		
	325	–6.360(2)	4.16(2)	–4.57(2)	7.01(2)		
	335	–15.026(2)	50.018(10)	–10.661(10)	16.86(2)		
<b>CHF<sub>3</sub></b>	<b>ZLI 1167<sup>[b]</sup></b>						
	300	–23.86(2)	39.604(15)	117.90(2)	–34.817(9)		
	305	–27.92(2)	46.218(9)	143.91(2)	–40.670(6)		
	310	–32.12(2)	53.018(8)	170.76(2)	–46.692(7)		
	315	–35.85(2)	59.038(9)	195.31(3)	–52.001(8)		
	320	–38.88(2)	63.960(8)	215.42(3)	–56.366(8)		
	325	–41.04(2)	67.367(9)	230.30(3)	–59.399(8)		
	330	–42.14(3)	69.043(10)	246.74(3)	–60.893(9)		
	335	–41.78(3)	68.447(12)	238.34(4)	–60.370(11)		
	339	–40.14(3)	65.533(13)	229.63(4)	–57.817(11)		
	342	–37.35(4)	60.998(9)	214.61(5)	–53.881(8)		

[a] Values in Hz with respect to the LC director. The standard deviations are given (in parenthesis) in units of the last digit. [b] The experimental values are multiplied by –2, because the director orients perpendicularly to the external magnetic field.

molecular geometry was only our secondary aim and, thus, we decided to use solvents that contain only certain type of functional groups (cyanide group both in ZLI 1132 and ZLI 1167, and di-azo group in the Phase V solvent), because the dissolved molecules were expected to be chemically active.

In the case of CH<sub>3</sub>F, the RMS minimum is flat but it very clearly excludes the possibility that the experimental  $\Delta^1J_{CF}$

would be over 350 Hz, where RMS increases rapidly. In the search for the RMS-minimum,  $\Delta^1J_{CF}$  was systematically changed and the molecular  $r_e$  geometry was iterated for each  $\Delta^1J_{CF}$  value. If we choose the value that gives the geometry closest to  $r_e$  given in reference [35], and simultaneously require an acceptable RMS value, the result of  $\Delta^1J_{CF} = 350$  Hz is obtained. The fitted molecular geometry is given in Table 3.

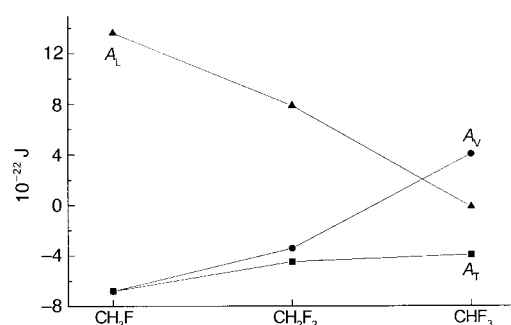


Figure 4. Principal components of the  $\mathbf{A}_{\text{CF}}$  tensors of  $\text{CH}_3\text{F}$ ,  $\text{CH}_2\text{F}_2$ , and  $\text{CHF}_3$  in the ZLI 1132 solvent at 300 K, 300 K, and 305 K, respectively. The terms  $A_V$  and  $A_T$  are perpendicular to ( $A_T$  in the local symmetry plane) and  $A_L$  parallel with the corresponding C-F bond. See text for details.

Table 12. Contributions to  $D^{\text{exp}}$  couplings for  $\text{CH}_3\text{F}$ ,  $\text{CH}_2\text{F}_2$  and  $\text{CHF}_3$  in the nematic ZLI 1132 solvent.<sup>[a]</sup>

Coupling	$D^{\text{eq}}$	$D^{\text{h}}$	$D^{\text{ah}}$	$D^{\text{d}}$	$1/2 J^{\text{aniso}}$	$D^{\text{calc}}$	$D^{\text{exp}}$	Diff. <sup>[b]</sup>
<b><math>\text{CH}_3\text{F}</math></b>								
$^1D_{\text{CF}}$	-856.07	-4.42	15.83	-1.22	9.45	-836.43	-836.42	0.01
$^1D_{\text{CH}}$	661.72	-20.74	-21.47	-8.43	0.16	611.24	611.24	0.00
$^2D_{\text{HF}}$	-678.77	2.14	18.99	2.01	-1.53	-657.16	-657.16	0.00
$^2D_{\text{HH}}$	859.60	-7.87	-28.38	-4.25	-0.28	818.82	818.82	0.00
<b><math>\text{CH}_2\text{F}_2</math></b>								
$^1D_{\text{CF}}$	-410.98	-1.17	4.28	-2.71	6.66	-403.92	-403.91	0.01
$^1D_{\text{CH}}$	914.02	-29.58	-24.01	6.46	0.18	867.07	867.06	-0.01
$^2D_{\text{HF}}$	-139.98	2.92	5.04	-1.09	-0.83	-133.94	-133.95	-0.01
$^2D_{\text{FF}}$	-460.28	-1.80	2.97	2.42	0.85	-455.84	-455.84	0.00
$^2D_{\text{HH}}$	1307.19	-17.98	-37.14	-1.37	-0.26	1250.44	1250.43	-0.01
<b><math>\text{CHF}_3</math></b>								
$^1D_{\text{CF}}$	71.78	-0.04	-1.66	-0.36	-1.12	68.60	68.55	-0.05
$^1D_{\text{CH}}$	-444.64	15.36	4.70	-39.99	-0.20	-464.77	-464.77	0.00
$^2D_{\text{HF}}$	-114.48	-0.70	2.45	0.00	0.26	-112.47	-112.56	-0.09
$^2D_{\text{FF}}$	102.71	0.32	-2.23	-0.30	-1.29	99.21	99.16	-0.05

[a] Values in Hz at 290, 290, and 287.5 K for the molecules in the respective order. [b]  $D^{\text{exp}} - D^{\text{calc}}$ .

Comparing the resulting molecular geometry for  $\text{CH}_2\text{F}_2$  with the microwave  $r_e$  geometry,<sup>[36]</sup> given also in Table 3, FCF bond angle is smaller in ZLI 1132 and ZLI 1167 solvents, whereas in Phase V the HCH bond angle is larger. In the latter case, also the  $r_{\text{CH}}$  bond length differs significantly from the microwave result. If the large change in the  $r_{\text{CH}}$  bond length is real, it should be reflected on the value of  $^1J_{\text{CH}}$ . The  $^1J_{\text{CH}}$  coupling values of the molecule in the LC solvents are 184.049(2) Hz, 183.95(5) Hz and 184.024(7) Hz (solvents in the same order as previously), which are very close to each other. Thus, the large change in  $r_{\text{CH}}$  is unlikely and the results obtained with the Phase V solvent should be treated with caution. However, the Phase V data did not affect our result for the indirect CF coupling tensor because the RMS error is nearly independent of  $\Delta^1J_{\text{CF}}$ . The clear minimum in the RMS of a joint fit to the experimental data in different LC solvents is seen at  $\Delta^1J_{\text{CF}} = 13.5$  Hz and  $J_{\text{CF,xx}} - J_{\text{CF,yy}} = -360$  Hz, which are relatively close to ab initio values, 10.39 and  $-280.33$  Hz. In the iteration of the experimental values, the ratio  $\Delta^1J_{\text{CF}} / (J_{\text{CF,xx}} - J_{\text{CF,yy}})$  was fixed to the corresponding ab initio result, because there was not enough information for both parameters to be determined independently. For the other couplings,  $\Delta J$  and  $J_{xx} - J_{yy}$  were fixed to the ab initio results, which thus

were used to produce the correction for the indirect contributions that are much smaller than in the  $^1D_{\text{exp}}^{\text{CF}}$  coupling. The analysis of the  $D^{\text{exp}}$  couplings is rather insensitive to the corrections due to the small  $J_{\text{aniso}}^{\text{ij}}$  contributions that, therefore, do not even have to be very accurate; a partial correction is enough.

In the case of  $\text{CHF}_3$ , we had to fix two geometry parameters. The choice between the ZLI 1132 or ZLI 1167 solvents did not have any remarkable effect on the bond lengths. For this reason, we found it quite safe to fix the  $r_{\text{CH}}$  and  $r_{\text{CF}}$  bond lengths to the ( $r_e$ ) values given in reference [37]. The resulting geometries corresponding to different solvents are given in Table 3. The deviation between the bond angle in the ZLI 1132 solvent and that given in reference [37] is only 0.5%. The RMS error is in this case most sensitive to  $\Delta^2J_{\text{FF}}$ , even though  $\Delta^1J_{\text{CF}}$  gives a slightly larger relative contribution to experimental couplings according to ab initio calculations. For this reason,  $\Delta^2J_{\text{FF}}$  was allowed to change whereas the other indirect coupling anisotropies were fixed to the ab initio values. The resulting experimental value,  $\Delta^2J_{\text{FF}} = -200$  Hz, is very close to the ab initio result,  $-232$  Hz.

**Significance of the anisotropic indirect coupling:** In Table 12, the  $D^{\text{ah}}$  contributions from anharmonic vibrations only serve to transform the molecular geometry from  $r_{\alpha}(T)$  to  $r_e$ . This is not essential in the studies of large molecules, for which the knowledge of the average geometry is adequate. The other contributions are, however, important, because they may lead to artificial results and poor fit to the data, if ignored. For example, the uncorrected  $D^{\text{exp}}$  couplings give the molecular geometry parameters of  $r_{\text{CH}} = 2.0615$  Å and  $\angle\text{HCF} = 111.88$  degrees for  $\text{CHF}_3$  in the ZLI 1132 solvent at 325 K, whereas the corrected values are 1.0958 Å and 110.92°, respectively. In this example, the dramatic effect is due to large  $^1D_{\text{CH}}$  contribution, which is seen also at 287.5 K in Table 12. However, it is also apparent that  $J^{\text{aniso}}$  gives the largest contribution to  $^1D_{\text{CF}}$  for each molecule and to  $^2D_{\text{FF}}$  for  $\text{CHF}_3$  (excluding the anharmonic corrections from the comparison).

The experimental and theoretical properties of the  $^1\mathbf{J}_{\text{CF}}$  tensor for  $\text{CH}_3\text{F}$  and  $\text{CH}_2\text{F}_2$  and of the  $^2\mathbf{J}_{\text{FF}}$  tensor for  $\text{CHF}_3$  are given in Table 13. The ratios,  $1/2 J^{\text{aniso}} / D^{\text{eq}}$ , are given in Table 14.

Table 13. Experimental and theoretical properties of the  $\mathbf{J}_{\text{CF}}$  tensor for  $\text{CH}_3\text{F}$  and  $\text{CH}_2\text{F}_2$  and of the  $\mathbf{J}_{\text{FF}}$  tensor for  $\text{CHF}_3$ .<sup>[a]</sup>

Molecule	Coupling	$J^{\text{iso}}$	$\Delta J$	$J_{xx} - J_{yy}$
$\text{CH}_3\text{F}$	$\mathbf{J}_{\text{CF}}$			
	exp.	-163.0 <sup>[b]</sup>	350	
	ab initio	-156.6	207.8	
$\text{CH}_2\text{F}_2$	$\mathbf{J}_{\text{CF}}$			
	exp.	-233.9 <sup>[b]</sup>	13.5 <sup>[c]</sup>	-360 <sup>[c]</sup>
	ab initio	-220.7	10.4	-280.3
$\text{CHF}_3$	$\mathbf{J}_{\text{FF}}$			
	exp.	- <sup>[d]</sup>	-200	
	ab initio	152.4	-232.1	

[a] Values in Hz and  $\mathbf{J}$  tensors expressed in the molecule-fixed ( $x, y, z$ ) frame. See text for details and Tables 8–10 for the tensors in their principal axis systems. [b] Measured in the gas phase. [c] The ratio,  $\Delta J / (J_{xx} - J_{yy})$ , is fixed to the value taken from ab initio results. [d] Not obtainable.

Table 14. Experimental and theoretical  $\frac{1}{2}J_{\text{CF}}^{\text{aniso}}$  contributions relative to the corresponding direct coupling,  $D^{\text{eq}}$ .<sup>[a]</sup>

Molecule	Method	CF	CH	HF	HH	FF
CH <sub>3</sub> F	ab initio	−0.7	0.02	0.2	−0.03	−
	Exp.	−1.1				
CH <sub>2</sub> F <sub>2</sub> <sup>[b]</sup>	ab initio	−1.2	0.02	0.6	−0.02	−0.02
	Exp.	−1.6				
CHF <sub>3</sub>	ab initio	−1.6	0.04	−0.2	−	−1.5
	Exp.					−1.3

[a] The relative contributions,  $\frac{1}{2}J_{\text{CF}}^{\text{aniso}}/D^{\text{eq}}$ , are given in %. [b] The values are orientation-dependent. The present values correspond to the data taken from ZLI 1132 solvent at 290 K.

For  ${}^1D_{\text{CF}}$ , the indirect contribution is close to  $-1\%$  in each case. For the corresponding contribution in *para*-difluorobenzene,<sup>[5]</sup> the experimental and theoretical results,  $-1.2\%$  and  $-1.1\%$ , respectively, are very similar to the present values. According to ab initio calculations,  ${}^1J_{\text{CF}}$  is almost cylindrically symmetric in the  $\mathbf{r}_{\text{CF}}$  direction, that is, in the  $(x', y', z')$  coordinate frame, where  $z'$  is in the bond direction. In this frame, the  ${}^1D_{\text{CF}}^{\text{eq}}$  coupling is directly proportional to  $S_{\text{CF}} = S_{z'z'}$  (see Equation (2)), whereas  ${}^1J_{\text{CF}}^{\text{aniso}}$  for CH<sub>2</sub>F<sub>2</sub> and CHF<sub>3</sub> consists of several terms of the general Equation (8):

$$J_{\text{aniso}} = \frac{3}{2}P_2(\cos\theta) [\Delta J S_{z'z'}^{\text{D}} + \frac{1}{2}(J_{x'x'} - J_{y'y'}) (S_{x'x'}^{\text{D}} - S_{y'y'}^{\text{D}}) + (J_{xy} + J_{yx}) S_{xy}^{\text{D}} + (J_{x'x'} + J_{z'z'}) S_{x'z'}^{\text{D}} + (J_{y'z'} + J_{z'y'}) S_{y'z'}^{\text{D}}] \quad (8)$$

because the direct and the indirect coupling tensors possess different principal axis systems. If we break the theoretical  ${}^1J_{\text{CF}}^{\text{aniso}}$  coupling into components, the first of which is directly proportional to  $S_{z'z'}$  (similarly to  ${}^1D_{\text{CF}}$ ) and the second includes the rest of the coupling, we obtain the contributions denoted  ${}^1J_{\text{CF,L}}^{\text{aniso}}$  and  ${}^1J_{\text{CF,T}}^{\text{aniso}}$ , respectively (L refers to “longitudinal” and T to “transverse”). The former reaches its maximum value when  $S_{\text{CF}} = 1$ . For example,  $\frac{1}{2}{}^1J_{\text{CF,L}}^{\text{aniso}} = 118.3$  Hz and  $\frac{1}{2}{}^1J_{\text{CF,T}}^{\text{aniso}} = 21.5$  Hz maximally for CHF<sub>3</sub>, with the latter value obtained using the constraint  $S_{\text{CF}} = 0$ , leading to vanishing dipolar coupling. Thus,  ${}^1D_{\text{CF}}^{\text{exp}}$  can be 21.5 Hz without any contribution from the true direct  ${}^1D_{\text{CF}}$  coupling. The corresponding values for  $\frac{1}{2}{}^1J_{\text{CF,L}}^{\text{aniso}}$  and  $\frac{1}{2}{}^1J_{\text{CF,T}}^{\text{aniso}}$  are 69.3 and 0 Hz for CH<sub>3</sub>F, 92.1 and 30.3 Hz for CH<sub>2</sub>F<sub>2</sub>, and 122.9 and 1.9 Hz for *para*-difluorobenzene. The values for the last molecule were calculated using theoretical results from reference [5]. The maximum of  ${}^1J_{\text{CF,L}}^{\text{aniso}}$  is seen to be much larger than  ${}^1J_{\text{CF,T}}^{\text{aniso}}$  for each molecule.  ${}^1J_{\text{CF,L}}^{\text{aniso}}$  gives a relative contribution that depends on the orientation similarly as  ${}^1D_{\text{CF}}^{\text{eq}}$  does; thus the relative contribution is orientation-independent. The orientation-independent ratios,  $\frac{1}{2}{}^1J_{\text{CF,L}}^{\text{aniso}}/{}^1D_{\text{CF}}^{\text{eq}}$ , are  $-1.1\%$ ,  $-0.6\%$  ( $-1.1\%$ ),  $-0.8\%$  ( $-1.0\%$ ), and  $-1.1\%$  ( $-1.2\%$ ), in the respective order of the molecules. The values in the parenthesis are the experimental results, which are presently not obtained for CHF<sub>3</sub>. As an implication, the  ${}^1J_{\text{CF}}^{\text{aniso}}$  contribution is partially removed by using the approximation,  $\frac{1}{2}{}^1J_{\text{CF}}^{\text{aniso}} \approx -{}^1D_{\text{CF}}^{\text{eq}}/100$ . However, if the order parameter  $S_{z'z'}$  is small compared with the other elements of the orientation tensor in the CF bond-fixed basis, the indirect contribution may deviate from the expected  $-1\%$ . In that case, the systematics of  ${}^1J_{\text{CF}}$  should be studied in related molecules in order to transform the complete tensor from a probe molecule to another.

In the case of  ${}^2D_{\text{FF}}^{\text{exp}}$ , the indirect contributions are about  $-0.02\%$  and  $-1.5\%$  in CH<sub>2</sub>F<sub>2</sub> and CHF<sub>3</sub>, respectively, according to the ab initio results. However, the former value is orientation-dependent, because the  ${}^2J_{\text{FF}}$  tensor deviates from cylindrical symmetry in the frame with  $z'$  parallel with  $\mathbf{r}_{\text{FF}}$ . On the contrary, the latter value is orientation-independent because of the symmetry point group of the molecule. In CH<sub>2</sub>F<sub>2</sub>, the relative indirect contribution,  $\frac{1}{2}{}^2J_{\text{FF,L}}^{\text{aniso}}/{}^2D_{\text{FF}}^{\text{eq}}$  is  $-0.8\%$ , which is partially cancelled by  $\frac{1}{2}{}^2J_{\text{FF,T}}^{\text{aniso}}$  in the observed  ${}^2D_{\text{FF}}^{\text{exp}}$ . If the  ${}^2D_{\text{FF}}^{\text{eq}}$  coupling should vanish in this molecule,  ${}^2J_{\text{FF,T}}^{\text{aniso}}$  would maximally equal 32.1 Hz ( ${}^2J_{\text{FF,T}}^{\text{aniso}}$  can reach the value of  $-48.1$  Hz if  $S_{z'z'}$  is not constrained to be zero and  ${}^2J_{\text{FF,L}}^{\text{aniso}}$  can be as much as 78.6 Hz at its maximum). The molecular orientation necessary for this coincidence is very strong:  $S_{z'z'} = 0$  and  $S_{x'x'} - S_{y'y'} = -1$  (where  $x'$  and  $y'$  correspond to the axes 1 and 2, given for  ${}^2J_{\text{FF}}$  in Table 9) that are realistic only in single-crystal studies, where the orientation of the molecule is defined by the orientation of the sample. Therefore, values of only a few Hz are possible for  $\frac{1}{2}{}^2J_{\text{FF,T}}^{\text{aniso}}$  in the LC-NMR method, whereas  $\frac{1}{2}{}^2J_{\text{FF,L}}^{\text{aniso}}/{}^2D_{\text{FF}}^{\text{eq}}$  is about  $-0.8\%$  and  $-1.5\%$  in CH<sub>2</sub>F<sub>2</sub> and CHF<sub>3</sub>, respectively.

Now we consider a case where the molecular orientation is not weak, but one internuclear order parameter, that is, one dipolar coupling vanishes leading to dominance of the corresponding indirect contribution  $J_{ij,\text{T}}^{\text{aniso}}$ . The negligible dipolar coupling corresponds to the situation where  $\mathbf{r}_{ij}$  is on the average at the magic angle ( $\approx 54.74^\circ$ ) with respect to  $\mathbf{n}$ . In the case of  $C_3$  or higher symmetry, the remaining  $J_{ij,\text{T}}^{\text{aniso}}$  contribution does not lead to serious errors, because small deviation of  $\mathbf{r}_{ij}$  from the magic angle leads to significant change of the dipolar coupling. Therefore, the fitted angle is insensitive to small errors that typically arise from the ignored  $J_{ij,\text{T}}^{\text{aniso}}$ . However, for less symmetric molecules, the property surface of the observed coupling with respect to a geometry parameter may be relatively flat. The situation arises occasionally from a suitable combination of the molecular geometry and orientation. In this case, even a small ignored contribution leads to significant errors. The possibility for the occurrence of the depicted situation is reduced significantly by carrying out measurements at several orientations and by fitting the free parameters simultaneously to the complete data set.

## Conclusions

We have performed multiconfiguration self-consistent-field linear response (MCSCF LR) calculations and liquid crystal (LC) NMR experiments in order to examine the spin–spin coupling tensors for CH<sub>3</sub>F, CH<sub>2</sub>F<sub>2</sub>, and CHF<sub>3</sub> molecules. The experimental tensorial data is found to be reproduced to a reasonable accuracy by the MCSCF calculations. The isotropic coupling constants are in excellent mutual agreement. The differences between the theoretical results and the experimentally very accurately determinable isotropic spin–spin coupling constants,  $J$ , are maximally only a few percent. Consistency in the anisotropies proves that both the theoretical and experimental methods used are able to produce reliable tensorial properties of the indirect couplings.

The present successful comparison of experimental and theoretical results strongly suggests that MCSCF calculations are able to produce qualitatively correct indirect contributions to the experimental dipolar couplings also for other small probe molecules containing fluorine. However, the convergence of the  $\mathbf{J}$  tensors necessitates very large MCSCF active spaces. Comparison of different theoretical results re-emphasizes that ab initio methods, such as the present one, are to be preferred over present density-functional theory in calculating couplings to fluorine, as anticipated for an atom containing lone pairs. The present theoretical data for the  $\mathbf{J}$  tensors are the best reported so far for these molecules.

The indirect contributions to the corresponding dipolar couplings due to  ${}^1\mathbf{J}_{\text{CF}}$  ( $\text{CH}_3\text{F}$  and  $\text{CH}_2\text{F}_2$ ) and  ${}^2\mathbf{J}_{\text{FF}}$  ( $\text{CHF}_3$ ) tensors are found both theoretically and experimentally to be negligible to a reasonable accuracy with the observed molecular orientations. However, especially the  ${}^2\mathbf{J}_{\text{FF}}$  tensor possesses low symmetry in the internuclear FF direction, which may lead to artificial effects on the apparent geometry and orientation of the molecule in the case of vanishing or nearly vanishing direct dipolar coupling. The relative indirect contribution to the  ${}^1D_{\text{CF}}^{\text{exp}}$  coupling from the  ${}^1\mathbf{J}_{\text{CF}}$  tensor is found to be rather similar in different structural surroundings and, therefore, it is partially removed by an average relative correction,  $-1\%$  of the corresponding dipolar coupling.

### Acknowledgement

The authors are grateful to the Academy of Finland for financial support. P.L. is grateful to the Finnish Cultural Foundation and to the Pohjois-Pohjanmaa Fund of the Finnish Cultural Foundation for grants. J.K. wants to express his gratitude to Finnish Cultural Foundation and Oulu University Foundation for grants. The computational resources were supplied by Center for Scientific Computing, Espoo, Finland.

- [1] J. Lounila, J. Jokisaari, *Progr. NMR Spectrosc.* **1982**, *15*, 249.
- [2] D. Sandström, K. T. Summanen, M. H. Levitt, *J. Am. Chem. Soc.* **1994**, *116*, 9357.
- [3] J. Kaski, J. Vaara, J. Jokisaari, *J. Am. Chem. Soc.* **1996**, *118*, 8879.
- [4] J. Kaski, P. Lantto, J. Vaara, J. Jokisaari, *J. Am. Chem. Soc.* **1998**, *120*, 3993.
- [5] J. Vaara, J. Kaski, J. Jokisaari, *J. Phys. Chem. A* **1999**, *103*, 5675.
- [6] K. W. Zilm, D. M. Grant, *J. Am. Chem. Soc.* **1981**, *103*, 2913.
- [7] M. L. Magnuson, L. F. Tanner, B. M. Fung, *Liq. Crystals* **1994**, *16*, 857.
- [8] M. L. Magnuson, B. M. Fung, M. Schadt, *Liq. Crystals* **1995**, *19*, 333.
- [9] T. R. Krugh, R. A. Bernheim, *J. Am. Chem. Soc.* **1969**, *91*, 2385; T. R. Krugh, R. A. Bernheim, *J. Chem. Phys.* **1970**, *52*, 4942.
- [10] J. Jokisaari, Y. Hiltunen, J. Lounila, *J. Chem. Phys.* **1986**, *85*, 3198.
- [11] J. B. S. Barnhoorn, C. A. de Lange, *Mol. Phys.* **1996**, *88*, 1.
- [12] S. Sýkora, J. Vogt, H. Bösigler, P. Diehl, *J. Magn. Reson.* **1979**, *36*, 53.
- [13] J. Lounila, R. Wasser, P. Diehl, *Mol. Phys.* **1987**, *62*, 19.
- [14] J. Lounila, P. Diehl, *J. Magn. Reson.* **1984**, *56*, 254; J. Lounila, P. Diehl, *Mol. Phys.* **1984**, *52*, 827; J. Lounila, *Mol. Phys.* **1986**, *58*, 897.
- [15] J. Jokisaari, "Anisotropy of shielding & coupling in liquid crystalline solutions" in *Encyclopedia of Nuclear Magnetic Resonance*, Vol. 2 (Eds.: D. Grant, R. Harris), Wiley, Chichester, **1996**, pp. 839–848.
- [16] H. Nakatsuji, H. Kato, I. Morishima, T. Yonezawa, *Chem. Phys. Lett.* **1970**, *4*, 607.
- [17] H. Nakatsuji, K. Hirao, H. Kato, T. Yonezawa, *Chem. Phys. Lett.* **1970**, *5*, 541.
- [18] H. Nakatsuji, I. Morishima, H. Kato, T. Yonezawa, *Bull. Chem. Soc. Jpn.* **1971**, *44*, 2010.
- [19] R. Ditchfield, L. C. Snyder, *J. Chem. Phys.* **1972**, *56*, 5823.
- [20] O. L. Malkina, D. R. Salahub, V. G. Malkin, *J. Chem. Phys.* **1996**, *105*, 8793.
- [21] R. M. Dickson, T. Ziegler, *J. Phys. Chem.* **1996**, *100*, 5286.
- [22] S. A. Perera, M. Nooijen, R. J. Bartlett, *J. Chem. Phys.* **1996**, *104*, 3290.
- [23] M. Nooijen, S. A. Perera, R. J. Bartlett, *Chem. Phys. Lett.* **1997**, *266*, 456.
- [24] O. Vahtras, H. Ågren, P. Jørgensen, H. J. Aa. Jensen, S. B. Padkjær, T. Helgaker, *J. Chem. Phys.* **1992**, *96*, 6120.
- [25] N. F. Ramsey, *Phys. Rev.* **1953**, *91*, 303.
- [26] P. Jørgensen, H. J. Aa. Jensen, J. Olsen, *J. Chem. Phys.* **1988**, *89*, 3654; J. Olsen, D. L. Yeager, P. Jørgensen, *Chem. Phys.* **1989**, *91*, 381.
- [27] T. Helgaker, M. Jaszuński, K. Ruud, A. Górska, *Theor. Chem. Acc.* **1998**, *99*, 175.
- [28] J. Guilleme, J. San Fabián, *J. Chem. Phys.* **1998**, *109*, 8168.
- [29] T. Helgaker, M. Jaszuński, K. Ruud, *Chem. Rev.* **1999**, *99*, 293.
- [30] T. Helgaker, H. J. Aa. Jensen, P. Jørgensen, J. Olsen, K. Ruud, H. Ågren, T. Andersen, K. L. Bak, V. Bakken, O. Christiansen, P. Dahle, E. K. Dalskov, T. Enevoldsen, B. Fernandez, H. Heiberg, H. Hettema, D. Jonsson, S. Kirpekar, R. Kobayashi, H. Koch, K. V. Mikkelsen, P. Norman, M. J. Packer, T. Saue, P. R. Taylor, O. Vahtras, *Dalton release 1.0, an electronic structure program*, **1997**. See <http://www.kjemi.uio.no/software/dalton/dalton.html>.
- [31] S. Huzinaga, *Approximate Atomic Functions*, University of Alberta, Edmonton, **1971**.
- [32] W. Kutzelnigg, U. Fleischer, M. Schindler in *NMR Basic Principles and Progress*, Vol. 23 (Eds.: P. Diehl, E. Fluck, H. Günther, R. Kosfeld, J. Seelig), Springer, Berlin, **1990**, pp. 165–262.
- [33] P.-O. Åstrand, K. V. Mikkelsen, P. Jørgensen, K. Ruud, T. Helgaker, *J. Chem. Phys.* **1998**, *108*, 2528.
- [34] H. J. Aa. Jensen, P. Jørgensen, H. Ågren, J. Olsen, *J. Chem. Phys.* **1998**, *88*, 3834.
- [35] T. Egawa, S. Yamamoto, M. Nakata, K. Kuchitsu, *J. Mol. Struct.* **1987**, *156*, 213.
- [36] E. Hirota, *J. Mol. Spectrosc.* **1978**, *71*, 145.
- [37] A. T. Maynard, R. E. Wyatt, *J. Chem. Phys.* **1995**, *103*, 8372.
- [38] J. A. Pople, M. Head-Gordon, K. Raghavachari, *J. Chem. Phys.* **1987**, *87*, 5968.
- [39] M. J. Frisch, G. W. Trucks, H. B. Schlegel, P. M. W. Gill, B. G. Johnson, M. A. Robb, J. R. Cheeseman, T. Keith, G. A. Petersson, J. A. Montgomery, K. Raghavachari, M. A. Al-Laham, V. G. Zakrzewski, J. V. Ortiz, J. B. Foresman, J. Cioslowski, B. B. Stefanov, A. Nanayakkara, M. Challacombe, C. Y. Peng, P. Y. Ayala, W. Chen, M. W. Wong, J. L. Andres, E. S. Replogle, R. Gomperts, R. L. Martin, D. J. Fox, J. S. Binkley, D. J. Defrees, J. Baker, J. P. Stewart, M. Head-Gordon, C. Gonzalez, J. A. Pople, *Gaussian 94, Revision B.1* (Gaussian, Inc., Pittsburgh PA, 1995).
- [40] R. Laatikainen, M. Niemitz, U. Weber, J. Sundelin, T. Hassinen, J. Vepsäläinen, *J. Magn. Reson. A* **1996**, *120*, 1.
- [41] R. Wasser, M. Kellerhals, P. Diehl, *Magn. Reson. Chem.* **1989**, *27*, 335.
- [42] Matlab Version 5.2.0.3084, see <http://www.mathworks.com>
- [43] C. E. Blom, A. Müller, *J. Mol. Spectrosc.* **1978**, *70*, 449.
- [44] S. Kondo, *J. Chem. Phys.* **1984**, *81*, 5945.
- [45] K. Kuchitsu, Y. Morino, *Bull. Chem. Soc. Japan* **1965**, *38*, 805.
- [46] J. Vaara, J. Lounila, K. Ruud, T. Helgaker, *J. Chem. Phys.* **1998**, *109*, 8388.
- [47] J. Vaara, Y. Hiltunen, *J. Chem. Phys.* **1997**, *107*, 1744.
- [48] K. Jackowski, W. T. Raynes, *J. Chem. Res. Synop.* **1977**, *3*, 66.
- [49] A. Smith, W. T. Raynes, *J. Cryst. Spectr. Res.* **1983**, *13*, 77.
- [50] V. G. Malkin, O. L. Malkina, D. R. Salahub, *Chem. Phys. Lett.* **1994**, *221*, 91.
- [51] J. Jokisaari, Y. Hiltunen, *Mol. Phys.* **1983**, *50*, 1013.

Received: June 10, 1999 [F 1840]